



---

# Selective fusion of structural and functional data for improved glaucoma detection

Paul Y. Kim<sup>1</sup>, Khan M. Iftakharuddin<sup>2</sup>, Pinakin G. Davey<sup>3</sup>, Martha Tóth<sup>4</sup>, Anita Garas<sup>4</sup>, Gabor Holló<sup>4</sup>, Edward A. Essock<sup>5</sup>

*<sup>1</sup>Department of Computer and Mathematical Sciences, Lewis University, Romeoville, IL, USA; <sup>2</sup>Department of Electrical and Computer Engineering, Old Dominion University, Norfolk, VA, USA; <sup>3</sup>College of Optometry, Western University of Health Sciences, Pomona, CA, USA; <sup>4</sup>Glaucoma Service, Department of Ophthalmology, Semmelweis University, Budapest, Hungary; <sup>5</sup>Department of Psychology and Brain Sciences, University of Louisville, KY, USA*

## Abstract

This work proposes a novel selective feature fusion of structural and functional data for improved glaucoma detection. The structural data, such as retinal nerve fiber layer (RNFL) thickness measurement acquired by scanning laser polarimetry (SLP), is fused with the functional visual field (VF) measurement recorded from the standard automated perimetry (SAP) test. The proposed selective feature fusion exploits the correspondence between structural and functional data obtained over multiple sectors. The correlation coefficients for corresponding structural-function sector pairs are used as weights in subsequent feature selection. The sectors are ranked according to the correlation coefficients and the first four highly-ranked sectors are retained. Following our prior work, fractal analysis (FA) features for both structural and functional data are obtained and fused for each of the selected sectors, respectively. These fused FA features are then used for glaucoma detection. The novelty of this work stems from (1) locating structure-functional sectoral correspondence; (2) selecting only a few interesting sector pairs using correlation coefficient between structure-function data; (3) obtaining novel FA features from these pairs; and (4) fusing these features for glaucoma detection. Such a method is distinctively different from other existing methods that exploit structure-function models in

---

**Correspondence:** Pinakin Davey OD PhD, College of Optometry, Western University of Health Sciences, Pomona, CA 91766, USA  
E-mail: [contact@pinakin-gunvant.com](mailto:contact@pinakin-gunvant.com)

---

that structure-function sectoral correspondences have been weighted and, based on such weights, only portions of the sectors are retained for subsequent fusion and classification of structural and functional features. For statistical analysis of the glaucoma detection results, sensitivity, specificity, and area under receiver operating characteristic curve (AUROC) are calculated. Performance comparison is obtained with those of existing feature-based techniques such as wavelet-Fourier analysis (WFA) and fast-Fourier analysis (FFA). Comparisons of AUROC values show that our novel selective feature fusion method for discrimination of glaucomatous and ocular normal patients slightly outperforms other existing techniques with AUROCs of 0.98, 0.98, and 0.99 for WFA, FFA, and FA, respectively.

*Keywords:* scanning laser polarimetry (SLP), standard automated perimetry, fusion, glaucoma detection, selective fusion, sectoral topographic correspondence, retinal nerve fiber layer (RNFL), fractal analysis (FA)

## 1. Introduction

Glaucoma is a progressive optic neuropathy which causes both structural and functional damages on eyes and ultimately leads to blindness.<sup>1</sup> Structural damages are due to rapid retinal ganglion cell death in the retinal nerve fiber layer (RNFL).<sup>2-4</sup> Functional damage is represented by visual field (VF) loss.<sup>5,6</sup> For a complete and reliable assessment of glaucomatous damages, it may be useful to consider both structural and functional visual impairment. Such a complete assessment may be more effective when the relationship between structure and function is known. It has been reported that local damage in the optic nerve corresponds to the regions of visual loss.<sup>7</sup> Such correspondences have been investigated, and models such as Hood-Kardon,<sup>8</sup> Harwerth,<sup>9</sup> Drasdo,<sup>10</sup> and Hockey-Stick<sup>11</sup> have been proposed. The Hood-Kardon model assumes that structural and functional data are linearly related. However, this assumption is only true for the peripheral rather than central visual field regions. Likewise, different regions may require different slopes or strengths. The Harwerth model is based on comparisons of perimetric data with histological data in monkey eyes, and has been validated with human histological data. However, the structure-function correspondence in the Harwerth model shows an increasing linearity with eccentricities, and yet does not accurately predict unique sectoral correspondences. The Drasdo model is a combination of both a linear and a non-linear relationship. Visual field sensitivities follow a linear relationship, whereas higher sensitivities follow a non-linear relationship. However, the non-linear part of the model may not have been well defined for accurate prediction. The Hockey-Stick model is a linear model with two different slopes, such as a shallower slope for the locations closer to fixation and a steeper slope for all other areas. However, only two slopes may not adequately represent the different structure-function relationship

of the regions. Overall, improved glaucoma detection based on structure-function correspondence has yet to be proven and verified.<sup>12-14</sup>

Research combining structural and functional data has reported better diagnostic power for glaucoma detection compared to using structural or functional data alone.<sup>15-18</sup> Horn *et al.* reported better glaucoma classification rates by simple addition of the scores from both structural and functional data.<sup>19</sup> However, a simple summation of structural and functional data in terms of scores cannot be an optimal method due to the lack of consideration of the unique structural-function relationship. Bizios *et al.* claimed 95% accuracy in glaucoma diagnosis by multiplying the different sectors for both structural and functional data with specific factors.<sup>20</sup> The factors were acquired by averaging pattern deviation probability scores based on six sectors. However, the authors did not report the AUROC performance metric for discriminating glaucoma.

Recently, Yousefi *et al.* reported a correlation-based feature subset selection where an optimal subset of the features was obtained by ranking all the features after concatenating 7 RNFL data points and 54 VF data points.<sup>21</sup> The correlation coefficients were measured between 61 individual points and the AUROC performance metric was obtained. However, the authors did not consider the unique correspondence between structural and functional data, which may provide an additional benefit for improved glaucoma detection.

In comparison, we propose a novel feature fusion method that exploits unique sectoral correspondence between structural and functional data in order to acquire better features. The proposed model selects multiple pair-wise sectors based on sectoral correspondences between structural and functional data, obtains correlation coefficients from pair-wise sectors, and selects the corresponding sector-pairs based on correlation coefficients, respectively. Finally, fractal analysis (FA) features are obtained from structural and functional data for selected sector-pairs and used in the subsequent feature fusion step. Our prior study shows the effectiveness of FA features in glaucoma detection.<sup>22</sup>

For functional data assessment, the original VF data, which are recorded in a circular 2D space with 59 data points, are converted into a 1D vector. For this step, the 59 data points are re-arranged with a novel labeling methodology, as discussed in a subsequent section. FA features are then extracted from the acquired functional data. For structural data assessment, both 1D and 2D RNFL eye-scan data are analyzed. For 1D RNFL assessment, a 1D temporal, superior, nasal, inferior, and temporal (TSNIT) graph consisting of RNFL thickness measurement data acquired by scanning laser polarimetry (SLP) around the parapapillary retina area is used. The FA features are extracted from the 1D TSNIT RNFL data. For 2D RNFL assessment, we investigate 2D feature-based techniques on specific regions of interest (ROIs) to represent glaucomatous damage. These ROIs are obtained around the parapapillary retina area excluding the optic disc. The maximum optic disc size is selected to ensure elimination of the optic disc.

Finally, selective feature fusion of the results is obtained from joint structural and functional analyses. For this task, a novel mapping table is obtained which divides the corresponding structural and functional data into ten sectors. Utilizing this mapping table, as shall be discussed in a subsequent section, the sector-wise correlation coefficients between structural and functional data are obtained. Such coefficients indicate the relative strength of correspondence between structural and functional data for each sector-pair, and are subsequently used as the global coefficients to weigh corresponding structural and functional data to emphasize the areas of significance in the sector-pairs. Following this step, only the sector-pairs with greater emphasis are retained. Fractal analysis (FA) features are then extracted from the selected sector-pairs of both structural and functional data. The FA features from structural and functional data are fused and classification performance metrics are obtained using the fused FA features for improved glaucoma detection.

Section 2 discusses a brief background review for functional, structural, and fractal analyses, as well as structure-function relationship. The detailed methodologies for the proposed techniques are discussed in Section 3. Results and corresponding discussion are presented in Section 4, followed by the conclusions in Section 5.

## 2. Background review

### 2.1. Functional analysis: visual field (VF) test

The VF is the area of space visible to central and peripheral vision in immobile eyes.<sup>6</sup> The VF test measures visual sensitivity in patients by evaluating their ability to detect points of light. Since patients may not recognize VF defects until the symptoms or signs of peripheral vision loss are obvious, the VF test can aid early detection of such defects. Standard automated perimetry has been widely used for testing VF. The VF test uses stationary white light stimuli at fixed locations on a white background, gradually increasing their intensity or size until the stimuli are perceived. The visibility at the fixed locations is measured using the threshold values of various intensities. The test is done one eye at a time and the patient is prompted to respond to light sensation. The threshold values are then recorded in the decibel (dB) scale, where zero dB denotes the brightest stimulus while the greatest dB is the dimmest stimulus.

### 2.1. Structural analysis: retinal nerve fiber layer (RNFL) assessment

Scanning laser polarimetry (SLP) is used for assessing RNFL data. SLP assesses ocular structure by estimating the thickness of the peripapillary RNFL based on its birefringent property.<sup>4</sup> When a polarized light reaches the birefringent structure of the RNFL, a phase-shift, *i.e.*, light retardation, occurs. The amount of retardation is directly proportional to RNFL thickness. Since the retardation can occur at the

cornea and lens, not just at the RNFL, proper compensation is necessary. After patient-specific compensation is performed, the amount of retardation is calculated pixel-wise and displayed in a map of the scanned area.

## **2.2 Wavelet-Fourier analysis (WFA)**

Complete details of the WFA analysis are available elsewhere.<sup>23</sup> Briefly, while fast-Fourier analysis (FFA) is a good candidate for analyzing non-stationary signals such as 1D TSNIT RNFL data, it has one drawback. In transforming to the frequency domain, the non-periodic local information is lost. Wavelet analysis (WFA) can overcome such a drawback by revealing the hidden aspects, such as breakdown points, discontinuities in higher derivatives, and self-similarity.<sup>23</sup> One major advantage of the WA is that it can perform local analysis, which analyzes a localized area of a larger signal using flexible wavelets. A wavelet is a waveform of effectively limited duration that has an average value of zero. Comparing wavelets in the WFA with the sinusoidal waves of the FFA, wavelets are more irregular and asymmetric with limited duration. For many signals, the low-frequency content is the most important part, providing the signal its identity. The high-frequency content, on the other hand, imparts unique characteristics. Hence, WFA has two filtering processes that obtain two different types of coefficients: approximation coefficients and detail coefficients. The approximation coefficients are the high-scale, low-frequency components of the signal. The detail coefficients are the low-scale, high-frequency components. These two processes constitute so-called wavelet decomposition. WFA is performed by applying a discrete-wavelet transform (DWT), resulting in the approximation and the detail coefficients.<sup>23</sup> A DWT is applied to the approximation coefficients to produce second-level results that are used in the subsequent analysis. The detail coefficients are processed using fast-Fourier transform (FFT) to obtain high-frequency information. The DWT and FFT are repeated on pre-determined scales using the amplitude to maximize performance.

## **2.3. Fast-Fourier analysis**

The discrete Fourier transformation breaks down a statistically varying signal into the elements of sinusoids of different frequencies so that it may transform the input signal from time-domain to frequency-domain. FFA is useful when the valuable information of the signal frequency is intended to be obtained and utilized. Mathematically, the process of FFA is represented by the Fourier transform, which is the sum over all time of the input signal, multiplied by a complex exponential.<sup>24</sup> In actual computer simulation, the Fourier transform is done in a discrete manner, yielding discrete Fourier coefficients. The fast-Fourier transform (FFT) is a computationally efficient implementation of the DFT that achieves the same results more quickly. Using these fast-Fourier coefficients, the composite function is obtained, allowing the constituent sinusoidal components of the original signal to be traced. In this study, the FFA is applied to the RNFL thickness data obtained from SLP.

## 2.4. Fractal analysis (FA)

A fractal is a rough or fragmented geometric object with an infinite nesting of structure at all scales. Each fractal is a reduced-size copy of the whole, which accounts for localized variation. In fractal analysis, the non-integer fractal dimension (FD) represents the quantitative measurement of the fractal object. For estimating FD, we use a box-counting (BC) and a multi-fractional Brownian motion (mBm) method. The BC method calculates the FD features for each size of the boxes by dividing a 2D image into boxes of predetermined size,  $r$ , and counting the number of the occupied boxes,  $N$ , needed to capture the signal values. The resulting FD features are the ratios between the logarithmic values of  $N$  and  $1/r$ . The mBm method calculates the FD features by adopting a continuous Gaussian process that measures a Holder exponent.

## 2.5. Structure-function relationships

A quantitative model relating structure (RNFL thickness or retinal ganglion cell (RGC) counts) and function (visual field sensitivity) is helpful in utilizing both structural and functional data for the diagnosis of glaucoma. The Hood-Kardon model is based on the linear structure-function relationship and predicts structural data (*i.e.*, RNFL thickness) from functional data (*i.e.*, visual field sensitivity). This model has shown limited accuracy due to the fact that the linear relationship holds for the peripheral visual field, whereas the relationship for the central visual field is non-linear. In addition, it has been shown that this model does not perform well in subjects with normal eyes. The Hockey-Stick model adopts two different relationships in two different regions that best describes the structure-function relationship. The first region involves the area surrounding the macula with a slope of 0.16, while elsewhere with a slope of 1. This two-line or Hockey-Stick model has provided a reasonable fit for all regions with the sharp breakpoint being smoothed or avoided. Recently, Yousefi *et al.* employed the concatenation of structural and functional features without consideration of any inherent structure-function relationship for feature fusion.<sup>21</sup> The structural features were obtained from ocular coherence tomography (OCT) RNFL thickness measurements, while functional features were the threshold values of the VF tests. Next, correlation-based feature subset selection (CFS) was used to select a subset of the best performing features out of a pool of features. The selected correlation coefficients were used to enhance the AUROC performance metric.

Unlike the models mentioned above, our proposed method considers the inherent structure-function relationship in multiple structural and functional regions. We obtain the relative importance of these structural-functional region pairs using correlation and retain only four pairs of regions for subsequent processing for glaucoma diagnosis.

### 3. Materials and methods

Figure 1 shows the overall flowchart of the proposed selective feature fusion method using fractal features from structural and functional test measurement data for improved glaucoma detection. In this study, we used 154 eyes (77 glaucomatous, 34 left-eyes, and 44 females; and 77 normal, 35 left eyes, and 51 females). Average age for these 154 patients was 57.06 with a standard deviation of 11.82. While approximately matched for age, the glaucomatous (mean age of 59.0) and normal (mean age of 55.1) patient groups showed a significant age difference (independent samples t-test  $t = -2.13$ ,  $P = 0.036$ ). We performed a statistical analysis by calculating sensitivity, specificity, and AUROC, and then compared the performance of the new method against that of existing feature-based techniques such as WFA and FFA. We briefly discuss each step in Figure 1.

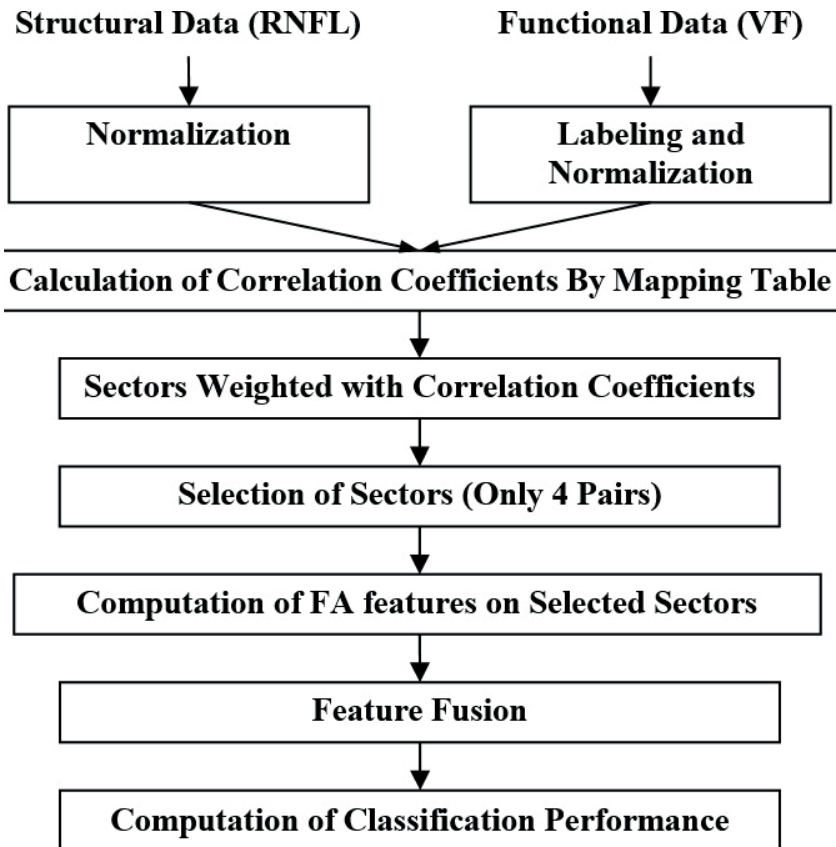


Fig. 1. Flowchart of a selective feature-based fusion method using fractal features from structural and functional test measurement data for glaucoma detection.

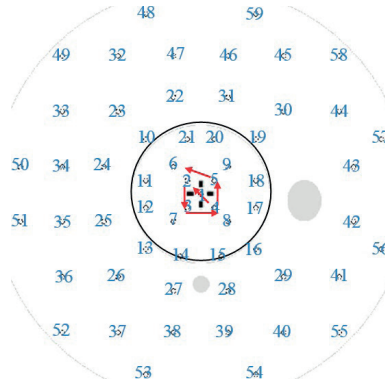


Fig. 2. The proposed labeling of visual field (VF) points in our work.

### 3.1. Functional analysis

The functional analysis begins by labeling the VF sensitivities at each of the 59 locations (Octopus Perimeter, Normal G2 program, Haag-Streit AG, Koeniz-Berne, Switzerland) using a novel labeling methodology. For the labeling methodology, all 59 VF points are arranged corresponding to the visual sensitivities into 1D data vectors by labeling and regrouping them using the following pre-determined labeling indices. Unlike other types of labeling, such as the raster scan method,<sup>25</sup> VF points are labeled clockwise for left eyes and counterclockwise for right eyes. This labeling is consistent with the one proposed by Holló *et al.*<sup>26</sup> Figure 2 shows the proposed labeling methodology of the 59 VF test points.

In Figure 2, the labeling starts from the center point and moves to the point that is located either at  $45^\circ$  for the left eye or  $135^\circ$  for the right eye. Subsequent points are followed clockwise for the left eye and counterclockwise for the right eye. Once the labeling is done, all the VF points of a specific patient are obtained in vector form. These VF data vectors are stacked together for all the patients.

### 3.2. Structural analysis

For 2D structural analysis, we obtain a region of interest (ROI) in a real 2D  $256 \times 128$  RNFL image data as follows. To obtain the best ROIs, we first obtain the square-shaped boxes that include the areas surrounding the optic disc. The squares that include the optic disc are excluded since the features from the optic disc do not contain useful information. The resulting outer box size is  $95 \times 95$ , while that for the inner box is  $47 \times 47$ . An example ROIs for a patient is shown in Figure 3. We then use the piecewise triangular prism surface area (PTPSA) method for FD feature extraction.<sup>27,28</sup>

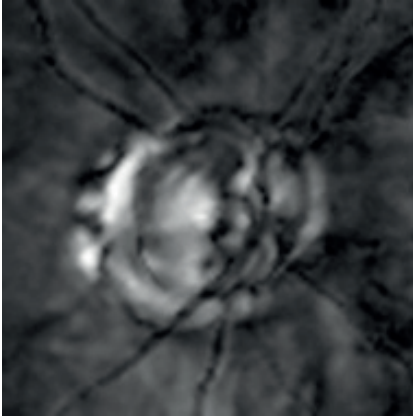


Fig. 3. An example of a patient (A) outer box ( $95 \times 95$ ) (B) inner box ( $47 \times 47$ ).

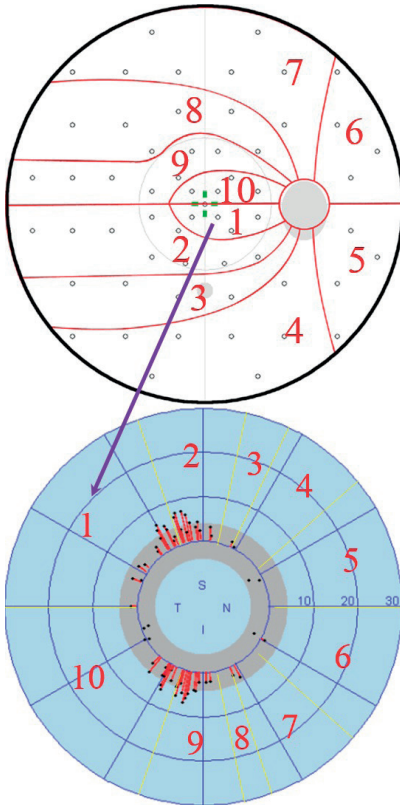


Fig. 4. VF sectors and their corresponding optic disc polar angle sectors.<sup>18</sup>

### 3.3. Selective feature-based fusion of structural and functional data

In this section, the sector-wise structural and functional relationship for selective feature fusion for improved glaucoma detection is discussed. Figure 4 shows a mapping between the 1D 64-point TSNIT RNFL data and 59 VF test points in ten sectors according to polar angle segmentation.<sup>29</sup> In order to show an example mapping, the 1<sup>st</sup> RNFL zone ( $0-70^\circ$ ) is associated with the four VF points in the 1<sup>st</sup> VF sector, as shown in Figure 4. Note that while polar angle analysis is done in a clock-wise way, the sectors are labeled in a counter-clock-wise way due to the fact that RNFL defects and VF defects are vertically mirrored. To ascertain the degree of association between the sectors of the 1D TSNIT RNFL and VF data, we obtain the scatter plots between the 1D TSNIT RNFL vs VF data for all 154 patients. We show a few out of the ten corresponding sectors in Figure 5. On each sector scatter plot, linear regression analysis has been performed to analyze the association between the 1D TSNIT RNFL and VF data.

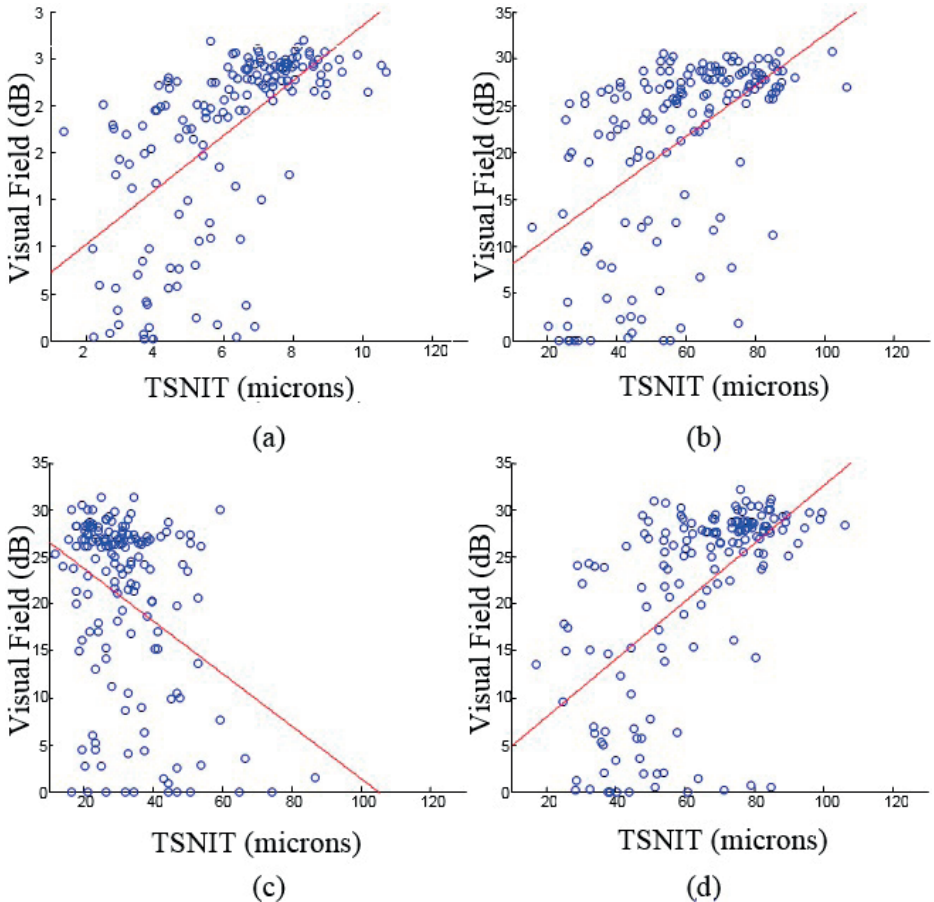


Fig. 5. Examples of scatter plots showing the association between the TSNIT measured by SLP and VF measured by SAP in each sector (2<sup>nd</sup>, 3<sup>rd</sup>, 8<sup>th</sup>, and 9<sup>th</sup>).

We then compute the degree of association for each sector using Pearson's correlation coefficients. Figure 6 shows the different degrees of association for the different sectors. The four sectors with the strongest associations based on Pearson's coefficients are selected. We then discard the information in the other sectors and utilize only the 2<sup>nd</sup>, 3<sup>rd</sup>, 8<sup>th</sup>, and 9<sup>th</sup> sectors that are weighted with the global coefficients, as shown in Figure 6. Therefore, we use 40% of the RNFL TSNIT and VF data for the rest of this study.

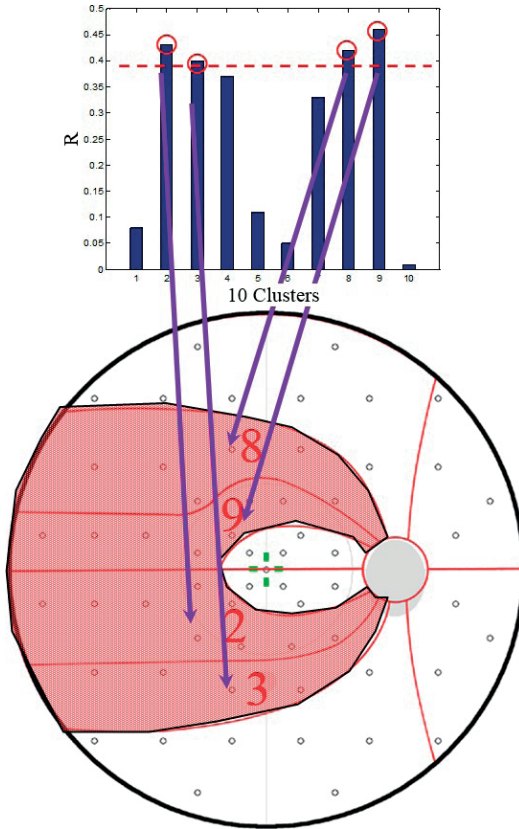


Fig. 6. Selected global coefficients for sectors and their corresponding VF sectors.

## 4. Results

### 4.1. Functional analysis

Figure 7 shows the VF data points from normal and glaucomatous eyes (right and left) for all 154 eyes. As discussed earlier, these VF data points have been labeled and plotted separately for comparison purposes.

Note in Figures 7b, 7d, 7f, and 7h that the right and left eyes in each group (*i.e.*, normal and glaucomatous eyes) have similar shapes, respectively. For normal eyes, as shown in Figures 7a and 7c, the plots show monotonically decreasing values without much variation. However, the shape of glaucomatous eyes has very different values than that of normal eyes, as shown in Figures 7(e) and (g), wherein there are considerable irregularities and abrupt changes. Such differences and changes in the shape of the VF data points between normal and glaucomatous eyes justify the use of feature-based techniques such as FFA, WFA, and FA.

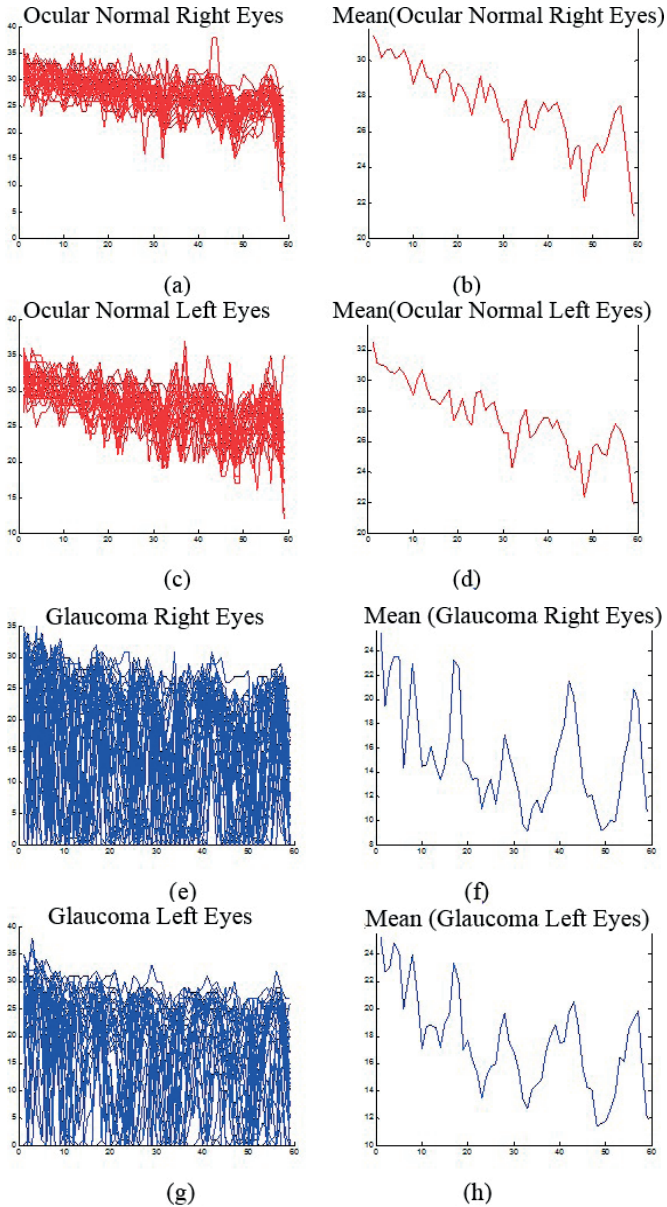


Fig. 7. 1D visual field (VF) raw threshold data in dB for normal and glaucoma eyes is plotted for the right and left eye separately: (a) normal right eyes; (b) mean value of normal right eyes; (c) normal left eyes; (d) mean value of normal left eyes; (e) glaucomatous right eyes; (f) mean value of glaucomatous right eyes; (g) glaucomatous left eyes; (h) mean value of glaucomatous left eyes.

Table 1. The comparison of sensitivity, specificity, and AUROC for functional analysis

<b>Methods</b>	(Sensitivity/Specificity/ <b>AUROC</b> ) (Sensitivity at 80; Sensitivity at 90)
<b>FFA</b>	0.84/0.99/ <b>0.87</b> (0.84; 0.84)
<b>WFA</b>	0.84/0.99/ <b>0.87</b> (0.84; 0.84)
<b>FA (BC + mBm)</b>	0.92/0.99/ <b>0.95</b> (0.92; 0.92)

Table 2. Comparison of AUROC for 1D TSNIT RNFL analysis

<b>Methods</b>	(Sensitivity/Specificity/ <b>AUROC</b> ) (Sensitivity at 80; Sensitivity at 90)
<b>FFA</b>	0.87/0.93/ <b>0.89</b> (0.87; 0.87)
<b>WFA</b>	0.87/0.93/ <b>0.91</b> (0.87; 0.87)
<b>FA</b>	0.90/0.92/ <b>0.91</b> (0.94; 0.73)

Table 3. AUROC comparison for real 2D RNFL analysis without optic disc

<b>Methods</b>	(Sensitivity/Specificity/ <b>AUROC</b> ) (Sensitivity at 80; Sensitivity at 90)
<b>FFA</b>	0.92/0.92/ <b>0.91</b> (0.95; 0.92)
<b>WFA</b>	0.88/0.87/ <b>0.91</b> (0.90; 0.81)
<b>FA</b>	0.92/0.90/ <b>0.92</b> (0.95; 0.90)

Table 1 shows the comparison of sensitivity, specificity, and AUROC for FFA, WFA, and FA for VF data analysis for all 154 patients. In Table 1, our fractal analysis (FA) feature-based technique performs the best among all feature-based techniques with corresponding AUROCs for FFA, WFA, and FA being 0.87, 0.87, and 0.95, respectively (FFA vs FA,  $P < 0.05$ ; WFA vs FA,  $P < 0.05$ ; FFA vs WFA,  $P < 0.05$ ). The best performance of fractal analysis features demonstrates that embedded irregularity in VF data has been well characterized.

Table 4. AUROC comparison of structural, functional data and their selective fusion for raw, FFA, WFA, and FA after the cluster-wise multiplication of Pearson's correlation coefficients

Methods	(Sensitivity/Specificity/AUROC) (Sensitivity at 80; Sensitivity at 90)			
	Structural (RNFL)	Functional (VF)	Fusion of all VF and RNFL data	Selective fusion of 40% VF and RNFL data
Raw	0.84/0.91/ <b>0.94</b> (0.92; 0.84)	0.78/0.99/ <b>0.92</b> (0.88; 0.79)	0.87/0.97/ <b>0.96</b> (0.92; 0.90)	0.96/0.90/ <b>0.98</b> (0.96; 0.95)
FFA	0.87/0.90/ <b>0.94</b> (0.90; 0.84)	0.78/0.96/ <b>0.92</b> (0.88; 0.79)	0.86/0.99/ <b>0.96</b> (0.96; 0.87)	0.96/0.94/ <b>0.98</b> (0.97; 0.96)
WFA	0.84/0.95/ <b>0.94</b> (0.88; 0.84)	0.84/0.99/ <b>0.94</b> (0.91; 0.86)	0.87/0.94/ <b>0.96</b> (0.94; 0.87)	0.94/0.94/ <b>0.98</b> (0.95; 0.94)
FA	0.81/0.91/ <b>0.90</b> (0.84; 0.81)	0.88/0.95/ <b>0.93</b> (0.88; 0.88)	0.92/0.94/ <b>0.98</b> (0.97; 0.92)	0.91/0.99/ <b>0.99</b> (1.00; 0.95)

The novel FA technique outperforms other feature-based techniques such as FFA and WFA by a margin of 8% in the functional analysis. However, comparison of our feature-based results with that of the mean deviation (MD) method suggests that the MD method shows an AUROC of 0.98 (does not differ significantly,  $P > 0.5$ ).

#### 4.2. Structural analysis

Using FA along with FFA and WFA features for 1D and 2D RNFL structural analyses yields the following results. Table 2 compares AUROC for 1D RNFL structural analysis, while Table 3 does the same for 2D RNFL structural analysis. We use the same PTPSA method for computing FD in this analysis. We then compute the AUROC that discriminates between glaucoma and normal patients with selected classifiers based on FFA, WFA, and FA features extracted from the ROIs of real 2D RNFL image data. Note that both 1D and 2D RNFL data analyses, even with our novel fractal features from real 2D RNFL image data, are not comparable to the 0.94 AUROC of the standard machine method known as the Nerve Fiber Index (NFI). There may be several reasons for this. First, literature review shows that real 2D RNFL images may not provide a better representation of glaucoma characteristics than 1D TSNIT RNFL. Second, we choose specific ROIs for real 2D analysis as square-shaped when the better representation may be circular-shaped. Since separate feature-based analyses of VF and RNFL data do not offer better glaucoma detection performance, we investigate fusion analysis for these data next.

### 4.3. Selective features-based fusion

For comparison, the AUROCs results for structural, functional, and selective feature fusion using raw data, FFA, WFA, and FA features are shown in Table 4, respectively. Table 4 shows that all simple fusion methods on raw data, FFA, WFA, and FA features enhance classification performance. The last column in Table 4 shows that the proposed selective fusion method using FA features slightly outperforms all feature-based and MD methods with an AUROC of 0.99. It should be noted that this improvement is obtained with only 40% of VF and RNFL data. It also outperforms the simple feature concatenation method (FA (BC + mBm)), whose accuracy is 95% ( $P < 0.05$ ).

## 5. Discussion

This study indicates the potential efficacy of selective feature fusion of structural and functional data for improved glaucoma detection. A novel labeling methodology is applied to VF data to obtain the 1D VF data vectors. Sophisticated FA features are extracted from both SF and structural RNFL data for selective feature fusion. The results in this paper show that the FA feature-based technique effectively exploits the shape features from VF data to perform as well or better than other feature-based techniques with corresponding AUROCs.

The efficacy of selective feature fusion of structural and functional data for improved glaucoma detection is demonstrated next. The proposed novel selective feature fusion exploits the inherent correspondence between RNFL and VF data using a lookup-type method. It is shown that selectively choosing 40% of the combined RNFL and VF data can effectively capture the inherent correspondence for improved glaucoma detection. Statistical analyses show that the proposed selective feature fusion method of structural and functional data does as well or better than existing WFA and FFA, with AUROCs of 0.98, 0.98, and 0.99, respectively.

Examining the application of shape-based analysis on the visual field data we find that the FA analysis outperforms the WFA and FFA by 8%; however, it is not superior at discrimination when compared to the MD as measured by visual fields. There are several possible reasons as to why our proposed feature-based results may not be as good as using the MD method. First, the patient group we studied may not reflect enough local variation or randomness in their original VF data (this will be considered in a future report). Hence, a global index such as MD performs well, whereas local feature-based techniques such as FFA, WFA, or FA may not perform as well. Second, even with the novel labeling methodology, the VF data vectors may not reflect structural information in the case of the RNFL. Consequently, performance may not be comparable. To address this issue, we utilize the topographic correspondence between structural and functional test measurement data to fuse useful information from both domains for improved glaucoma detection.

Yousefi *et al.*<sup>21</sup> has recently published a study combining structure and function results. They acquired a total of 61 features: 7 points (6 RNFL sectoral data points plus 1 global metric) from structural data and 54 points from functional SAP data. Different machine-learning classifiers, such as Bayesian network, are applied to the concatenated data. Unlike the simple concatenation of raw structural and functional data used as input features in Yousefi *et al.*,<sup>21</sup> the features in this study are combined considering inherent structural-functional regional correspondence. Furthermore, the current study obtains sophisticated FD from both structural and functional data. The authors in Yousefi *et al.*<sup>21</sup> focused on comparing the longitudinal progression of glaucoma by obtaining differentials of the time-relapsed data. In comparison, our focus in this work has been differentiating between glaucomatous and normal eyes by exploiting the inherent structural-functional relationship. Yousefi *et al.*<sup>21</sup> have found the correlation coefficients against the discriminating power, thus ranking all 61 features from highest to lowest. They further conclude that retaining the ten best features offers the best AUROC (0.88) for discriminating progressive glaucoma from stable patients. In comparison, the proposed selective feature fusion method in this study retains four corresponding structure-functional sectors based on the highest correlation coefficients that reflect inherent correspondence. This structure-functional correspondence may best exploit the topographic sector-wise relationship of the structural and functional data, unlike the work reported in Yousefi *et al.*<sup>21</sup>

Glaucoma diagnosis and management are both facilitated and complicated by the various structural and functional methods available for ocular evaluation. Obtaining and unifying data and cross-confirmation of structural and functional results can indeed help to improve diagnostic ability and may have an application in detecting progression. In this study, we have developed techniques that can combine retinal nerve fiber layer data and visual field data to one unified classifier. It is relatively simple to use these shape-based techniques in devices that measure the nerve fiber layer. The results in the present and previous studies show that glaucoma diagnosis and progression detection can be improved using these methods. Manufacturers could consider applying these methods to the data and produce output that may benefit the clinical use of these devices. In our future work, patient-specific structure-functional relationship may be exploited for selective feature selection rather than group-wise processing, as has been done in this study. Now that these methods have been implemented and their potential demonstrated, future research will compare them more rigorously using cross-validation methods and distinct samples. Furthermore, for improved processing of real 2D structural image data, we plan to investigate circular-shaped ROIs that may provide better diagnostic capability for glaucoma detection.

## References

1. Weinreb, R. N. and Khaw, P. T., Primary open angle glaucoma, *Lancet*, 363, 1711-1720 (2004).
2. Garway-Heath, D. F., Caprioli, J., Fitzke, F. W. and Hitchings, R. A., Scaling the hill of vision: the physiological relationship between light sensitivity and ganglion cell numbers, *Invest Ophthalmol Vis Sci.*, Vol. 41, pp. 1774-1782, (2000).
3. Quigley, H. A., Miller, N. R. and George, T., Clinical evaluation of nerve fiber layer atrophy as an indicator of glaucomatous optic nerve damage, *Arch Ophthalmol*, 98, 1564-1571 (1980).
4. Quigley, H. A. and Addicks, E. M., Quantitative studies of retinal nerve fiber layer defects," *Arch Ophthalmol*, 100, 807-814 (1982).
5. Lauande-Pimentel, R., Carvalho, R. A., Oliveira, H. C., Gonçalves, D. C., Silva, L. M., and Costa, V. P., Discrimination between normal and glaucomatous eyes with visual field and scanning laser polarimetry measurements, *Br. J. Ophthalmol*. 85, 586-591, (2001).
6. Dersu, I. and Wiggins, M. N., Understanding Visual Fields, Part II; Humphrey Visual Fields, *J. of Ophthalmic Medical Technology*, 2(3), (2006).
7. Hood, D. and Kardon, R. H., A framework for comparing structural and functional measures of glaucomatous damage," *Prog Retin Eye Res.*, 26(6), 688-710 Nov. (2007).
8. Hood, D., Anderson, S. C., Wall, M., Randy, H. and Kardon, R. H., Structure versus Function in Glaucoma: An Application of a Linear Model, *Invest. Ophthalmol. Vis. Sci.*, 48(8), 3662-3668 Aug. (2007).
9. Harwerth, R. S., Wheat, J. L., Fredette, M. J., Anderson, D. R., Linking structure and function in glaucoma, *Prog Retin Eye Res.*, 29(4), 249-71 (2010).
10. Drasdo, N., Mortlock, K. E., North, R. V., Ganglion cell loss and dysfunction: relationship to perimetric sensitivity, *Optom Vis Sci*. 85(11), 1036-1042 (2008).
11. Malik, R., Swanson, W. H., Garway-Heath, D. F., Structure-function relationship' in glaucoma: past thinking and current concepts, *Clin Experiment Ophthalmol*, 40(4), 369-80 (2012).
12. Garway-Heath, D. F., Holder, G. E., Fitzke, F. W., and Hitchings, R. A., Relationship between electrophysiological, psychophysical, and anatomical measurements in glaucoma. *Invest Ophthalmol Vis Sci.*, 43(7), 2213-20. (2002).
13. Reus, N. J. and Lemij, H. G., The relationship between standard automated perimetry and GDx VCC measurements, *Invest Ophthalmol Vis Sci*. 45(3), 840-5 (2004)
14. Sherman, J. Slotnick, S. and Boneta, J., Discordance between structure and function in glaucoma: Possible anatomical explanations, *Optometry*, 80, 487-501 (2009).
15. Horn, F. K., Mardin, C. Y., Laemmer, R., Baleanu, D., Juenemann, A. M., Kruse, F. E. and Tornow, R. P., Correlation between Local Glaucomatous Visual Field Defects and Loss of Nerve Fiber Layer Thickness Measured with Polarimetry and Spectral Domain OCT, *Invest Ophthalmol Vis Sci.*, 50(5), 1971-1977, May. (2009).
16. Strouthidis, N. G., Vinciotti, V., Tucker, A. J., Gardiner, S. K., Crabb, D. P., and Garway-Heath, D. F., Structure and Function in Glaucoma: The Relationship between a Functional Visual Field Map and an Anatomic Retinal Map, *Invest. Ophthalmol. Vis. Sci.*, Vol. 47(12), pp. 5356-5362, Dec., (2006).
17. Danesh-Meyer, H. V., Ku, J. Y. F., Papchenko, T. L., Jayasundera, T., Hsiang, J. C. and Gamble, G. D., Regional Correlation of Structure and Function in Glaucoma, Using the Disc Damage Likelihood Scale, Heidelberg Retina Tomograph, and Visual Fields, *Ophthalmology*, 113(4), 603-611, Apr. (2006).
18. Shah, N. N., Bowd, C., Medeiros, F. A., Weinreb, R. N., Sample, P. A., Hoffmann, E. M. and Zangwill, L. M., Combining Structural and Functional Testing for Detection of Glaucoma, *Ophthalmology*, 113, 1593-1602 (2006).
19. Horn, F. K., Mardin, C. Y., Bendschneider, D., Jünemann, A. G., Adler, W., and Tornow, R. P., Frequency doubling technique perimetry and spectral domain optical coherence tomography in patients with early glaucoma, *Eye (Lond)*. 25(1), pp. 17-29 (2011).

20. Bizios, D., Heijl, A., and Bengtsson, B., Integration and fusion of standard automated perimetry and optical coherence tomography data for improved automated glaucoma diagnostics, *BMC Ophthalmology*, 11(20) (2011).
21. Yousefi, S., Goldbaum, M. H., Balasubramanian, M., Jung, T. P., Weinreb, R. N., Medeiros, F. A., Zangwill, L. M., Liebmann, J. M., Girkin, C. A. and Bowd, C., Glaucoma Progression Detection Using Structural Retinal Nerve Fiber Layer Measurements and Functional Visual Field Points, *IEEE Trans. On Biomedical Engineering*, 61(4), 1143-1154 (2014)
22. Kim, P. Y., Iftekharuddin, K. M., Davey, P. G., Tóth, M., Garas, A., Holló, G. and Essock, E. A., Novel Fractal Feature-Based Multiclass Glaucoma Detection and Progression Prediction, *IEEE Jour. of Biomedical and Health Informatics*, 17(2), 269-276 (2013)
23. Essock, E. A., Zheng, Y. and Gunvant, P., Analysis of GDx-VCC Polarimetry Data by Wavelet-Fourier Analysis across Glaucoma Stages, *Invest Ophthalmol Vis Sci*, 46(8) Aug. (2005).
24. Essock, E. A., Sinai, M. J., Fechtner, R. D., Srinivasan, N. and Bryant, F. D., Fourier Analysis of nerve fiber layer measurements from scanning laser polarimetry in glaucoma: emphasizing shape characteristics of the 'doublehump' pattern, *J Glaucoma* 9, 444-452 (2000).
25. Ferreras, A., Pablo, L. E., Garway-Heath, D. F., Fogagnolo, P., and Garcia-Feijoo, J., Mapping Standard Automated Perimetry to the Peripapillary Retinal Nerve Fiber Layer in Glaucoma, *Invest. Ophthalmol. Vis. Sci.*, Vol. 49 (7), pp. 3018-3025, Jul., (2008).
26. Holló, G, Naghizadeh, F., Evaluation of Octopus Polar Trend Analysis for detection of glaucomatous progression, *Eur J Ophthalmol* (2014), DOI: 10.5301/ejo.5000504.
27. Ahmed, S. and Iftekharuddin, K. M., Discrimination of medulloblastoma and low grade astrocytoma PF tumors using selected MR image features, *MemBis 2008*, (2008).
28. Zook, J. M. and Iftekharuddin, K. M., Statistical analysis of fractal-based brain tumor detection algorithms, *Magnetic Resonance Imaging*, 23, 671-678 (2005).
29. EyeSuite Application Note, Follow up from HFA with Octopus <https://www.haag-streit.com/haag-streit-diagnostics/products/perimetry/> accessed 08/08/2016